Production of isotopes near the heavy-element nucleosynthesis path at FRS

Downloaded from: https://research.chalmers.se, 2026-10-17 03:32 UTC

Citation for the original published paper (version of record):
Pietri, S., Rösch-Kabadayı, H., Enders, J. et al (2026). Production of isotopes near the heavy-element nucleosynthesis path at FRS. Physics Letters, Section B: Nuclear, Elementary Particle and High-Energy Physics, 880. http://dx.doi.org/10.1016/j.physletb.2026.140729

N.B. When citing this work, cite the original published paper.

research.chalmers.se offers the possibility of retrieving research publications produced at Chalmers University of Technology. It covers all kind of research output: articles, dissertations, conference papers, reports etc. since 2004. research.chalmers.se is administrated and maintained by Chalmers Library

(article starts on next page)

Phys. Lett. B 880 (2026) 140729

Contents lists available at ScienceDirect

Physics Letters B

journal homepage: www.elsevier.com/locate/physletb

Letter

Production of isotopes near the heavy-element nucleosynthesis path at FRS

S. Pietri [a,*], H.A. Rösch-Kabadayı [a,b,c], J. Enders [b,c], T. Grahn [d,e], J.-P. Hucka [b,c], T. Kurtukian-Nieto [f,g], M. Luoma [d,e], A. M. Bruce [h], T. Dickel [a,i], E. Haettner [a], C. Hornung [a], D. Kostyleva [a], W. R. Plaß [a,i], H. Weick [a], J. Wirtz [a,b], J. Zhao [a], H. M. Albers [a], D. Amanbayev [a,c,i], S. Ayet San Andres [j], J. Äystö [d,e], S. Bagchi [a,1], S. Beck [a,i], J. Benlluire [k], J. Bergmann [i], Z. Brencic [l,m], H. Geissel [a,2], F. Greiner [a], L. Gröf [i], M. N. Harakeh [n], A. Heinz [o], C. E. Jones [h,3], N. Kalantar-Nayestanaki [n], A. Kankainen [d,e], A. Kelic-Heil [a], B. Kindler [a], G. Kripko-Koncz [c,i,4], N. Kuzuminchuk [a], B. Lommel [a], K. Mahajan [c,i], I. Miskun [i], A. Mistry [a], A. Mollaebrahimi [a,i], I. Mukha [a], G. Münzenberg [a,2], M. Pfützner [p], Zs. Podolyák [q], S. Purushotaman [a], C. Rappold [f], P. H. Regan [q,r], J. L. Rodríguez-Sánchez [k,5], C. Scheidenberger [a,c,i], H. Simon [a], J. Taieb [s,t], Y. K. Tanaka [a,u], H. Törnqvist [a], M. Vencelj [l], J. Vesic [l], J. S. Winfield [a,2], M. Winkler [a],
(for the Super-FRS Experiment Collaboration)

[a] GSI Helmholtzzentrum für Schwerionenforschung, Darmstadt, 64291, Germany
[b] Institut für Kernphysik, Fachbereich Physik, Technische Universität Darmstadt, Darmstadt, 64289, Germany
[c] Helmholtz Forschungsakademie Hessen für FAIR, Darmstadt, 64291, Germany
[d] University of Jyvaskyla, Department of Physics, P.O. Box 35, Jyvaskyla, FI-40014, Finland
[e] Helsinki Institute of Physics, P.O. Box 64, Helsinki, FI-00014, Finland
[f] Instituto de Estructura de la Materia (IEM), CSIC, Madrid, 28006, Spain
[g] Laboratoire de Physique des deux Infinis Bordeaux, Université de Bordeaux, Gradignan, 33170, France
[h] School of Architecture, Technology and Engineering, University of Brighton, Brighton, BN2 4GJ, United Kingdom
[i] II. Physikalisches Institut, Justus-Liebig-Universität Gießen, Gießen, 35392, Germany
[j] Institut de Física Corpuscular, Universitat de Valencia, Paterna, 46980, Spain
[k] IGFAE, Universidade de Santiago de Compostela, Santiago de Compostela, 15782, Spain
[l] Jožef Stefan Institute, Ljubljana, 1000, Slovenia
[m] University of Ljubljana, Ljubljana, 1000, Slovenia
[n] Energy and Sustainability Research Institute Groningen, Rijksuniversiteit Groningen, Groningen, 9747 AA, the Netherlands
[o] Department of Physics and Astronomy, Chalmers Tekniska Högskola, Gothenburg, 412 96, Sweden
[p] Faculty of Physics, University of Warsaw, Warszawa, 02-093, Poland
[q] School of Mathematics and Physics, University of Surrey, Guildford, GU2 7XH, United Kingdom
[r] National Physical Laboratory, Teddington, Middlesex, TW11 0LW, United Kingdom
[s] CEA DAM Île de France, Bruyères-le-Châtel, Arpajon cedex, 91297, France
[t] Laboratoire Matière en Conditions Extrêmes, Université Paris-Saclay, Bruyères-le-Châtel, 91680, France
[u] High Energy Nuclear Physics Laboratory, RIKEN, Wako, Saitama, 351-0198, Japan

* Corresponding author.
E-mail addresses: S.Pietri@gsi.de (S. Pietri), H.Roesch@gsi.de (H.A. Rösch-Kabadayı).
[1] Current address: Department of Physics, IIT-ISM Dhanbad, Jharkhand 826004, India
[2] Deceased
[3] Current address: School of Mathematics and Physics, University of Surrey, Guildford GU2 7XH, United Kingdom
[4] Current address: School of Physics and Astronomy, University of Edinburgh, EH9 3FD, United Kingdom
[5] Current address: CITENI, Campus Industrial de Ferrol, Universidade da Coruña, E-15403 Ferrol, Spain

https://doi.org/10.1016/j.physletb.2026.140729
Received 13 March 2026; Received in revised form 6 July 2026; Accepted 6 July 2026
Available online 9 July 2026
0370-2693/© 2026 The Author(s). Published by Elsevier B.V. Funded by SCOAP³. This is an open access article under the CC BY license (http://creativecommons.org/licenses/by/4.0/).

ARTICLE INFO

Editor: Silvia Monica Lenzi

Keywords:
r-process
Nucleosynthesis
Fragmentation reactions
Isotope discovery

ABSTRACT

Neutron-rich isotopes far from stability were produced and observed at the projectile Fragment Separator (FRS) of the GSI Helmholtzzentrum für Schwerionenforschung in the FAIR Phase-0 experimental program. The isotopes were produced in April 2020 in the fragmentation of a 1.05 GeV/nucleon ^{208}Pb beam on a beryllium target. The experiment targeted the neutron-rich region near the $N = 126$ shell closure, a key area for understanding the astrophysical *r*-process, but largely unexplored due to the experimental challenges in producing such exotic nuclei. Within this work, we identified five isotopes which were not seen previously at FRS; ^{184}Tm, ^{195}Ta, ^{198}W, ^{200}Re, and ^{201}Re — the latter located directly on the $N = 126$ line. These observations corroborate the extension of the nuclear chart and highlight the capabilities of the FRS and of in-flight fragmentation at relativistic energies in accessing this region.

1. Introduction

Heavy neutron-rich isotopes of atomic nuclei lighter than ^{208}Pb play a key role in our understanding of the formation of heavy elements in the universe. Approximately half of the isotopes of elements heavier than iron are produced by the rapid neutron capture process (*r*-process [1,2]), and the elements heavier than bismuth are produced exclusively by it. For instance, the isotopes of uranium that are important for energy production would not exist without the *r*-process. Evidence of this process was gathered in simultaneous observations of gravitational waves and electromagnetic signals from the binary neutron-star merger event [3]. Such a remarkable observation sparked a quest to probe the *r*-process nucleosynthesis in more detail. The precise location of the *r*-process path in the Segré chart depends on the neutron flux and, for a given element, on the balance between average neutron-capture times and β-decay half-lives. The nuclear-physics parameters defining which isotopes are involved in the process are the mass excess of the isotopes and their β-decay half-lives (see refs. [4,5] and references therein). To study these properties it is necessary to produce the nuclei involved in the laboratory. Along the *r*-process path, nuclei close to the neutron number $N = 126$ have been a subject of increasing interest in recent years. Since $N = 126$ forms a closed neutron shell, this neutron number marks a series of waiting points in the *r*-process, causing matter to build up around $N = 126$. This effect, generated by the shell structure, leads to a so-called third *r*-process peak in the solar system isotopic abundance curve.

Consequently, any indication of a change in the shell structure for very neutron-rich systems, as has been found in light nuclei [6], may affect the nucleosynthesis pattern and should be investigated experimentally. The chart of nuclei south of ^{208}Pb is largely unexplored. The lightest $N = 126$ isotone that has been identified up to date is ^{202}Os [7]. Heavy nuclei along the *r*-process path are challenging to produce in the laboratory since the fission of uranium isotopes does not produce nuclides with masses $A \gtrsim 160$ and with $A/Z > 2.6$ with sufficient yields. A universal method to produce neutron-rich heavy nuclei is projectile fragmentation, where a heavy nucleus (for example, ^{208}Pb or ^{238}U) is forced to break into lighter nuclei through a collision at high energy. In peripheral collisions, neutron-rich nuclides are accessible when mainly protons are abraded from the heavy nucleus, and the excitation energy of the reaction residue remains low, so that few or even no neutrons evaporate [8,9]. At beam energies greater than several hundred MeV per nucleon, charge-changing reactions via isobaric excitations may lead to even more exotic nuclei [10], although at lower cross section. The collection of nuclides is efficient when the collision partner undergoing cold fragmentation moves at high velocity, i.e.,in the case of in-flight fragmentation. Here, magnetic separators can be used to capture a large fraction of the fragmentation yield in the forward direction and to perform event-by-event identification. In addition to projectile fragmentation, another method that is under development is the multi-nucleon transfer reaction that has already contributed to isotope discovery in the actinide region [11]. In this Letter, we report on the production and identification of five previously unobserved isotopes at or near the $N = 126$ shell closure using in-flight fragmentation of ^{208}Pb at relativistic energies. Our experiment ran in April 2020 and during the submission process of this letter the authors were made aware of the work of Fukuda et al. [12], which includes the identification of those five isotopes.

2. Experimental details

Neutron-rich isotopes close to the $N = 126$ shell closure were produced, separated and identified at the Fragment Separator (FRS [13]) of the GSI Helmholtzzentrum für Schwerionenforschung, Darmstadt (Germany) within the FAIR Phase-0 experimental program. The SIS-18 synchrotron provided ^{208}Pb primary beam of 1.05 GeV/nucleon at intensities up to 1.5×10^9 ions/spill and spill lengths of 1–10 seconds at a repetition rate of 3–12 seconds. The fragmentation products produced in the 4 g/cm^2 thick beryllium target at the entrance of the FRS were separated in-flight using an achromatic ion-optical mode. A 225 mg/cm^2 thick niobium backing of the target ensured that the fragmentation products were almost all completely ionized, which aided their identification and transmission. An aluminium degrader wedge with variable angle was used at the dispersive focal plane F2 providing spatial separation of fragments at the final focal plane F4. The detector systems and magnets of FRS are depicted schematically in Fig. 1.

The unambiguous identification of fragments was achieved by the event-by-event measurement of their electric charge, Q, and mass number, A using the $B\rho - \Delta E - TOF$ method [13]. For the charge measurement, two Multiple Sample Ionization Chambers (MUSIC [14]) filled with P10 gas were used to measure the energy loss (ΔE) of ions at F4. A niobium foil was installed between the two detectors to ensure efficient stripping of the ions.

The mass number A was derived from magnetic rigidity ($B\rho$) analysis and time-of-flight (TOF) measurements that led to the mass-over-charge ratio (A/Q). For this, two Time Projection Chambers (TPC [15]) were used at F2 and F4 each, to track the trajectories of the fragments, and ultimately determine their $B\rho$. The time-of-flight between F2 and F4 was measured using plastic scintillator detectors. A path-length correction, based on the ion-optical matrix of the second half of the FRS, was applied to the resulting mass-to-charge ratios. Adjusting the thickness of the degrader at F4, the isotopes were implanted either in the FRS Ion Catcher [16] for atomic mass measurement or in the active stopper [17], for lifetime measurement. Such a setup permits the measurement of the *r*-process relevant quantities, β-decay half lives, masses and isotope identification in a single experiment. When implanting the ions at F4, the mean-range bunching technique described in ref. [18], was used.

Following initial calibration runs with the ^{208}Pb primary beam, the FRS magnets were subsequently tuned to four separate fragment settings, to centre the fully ionised ^{205}Au, ^{193}W, ^{193}Ta, and ^{190}Lu and ensure the unequivocal identification of previously unobserved nuclides. The previously unidentified isotopes were all observed in the setting centred on ^{190}Lu.

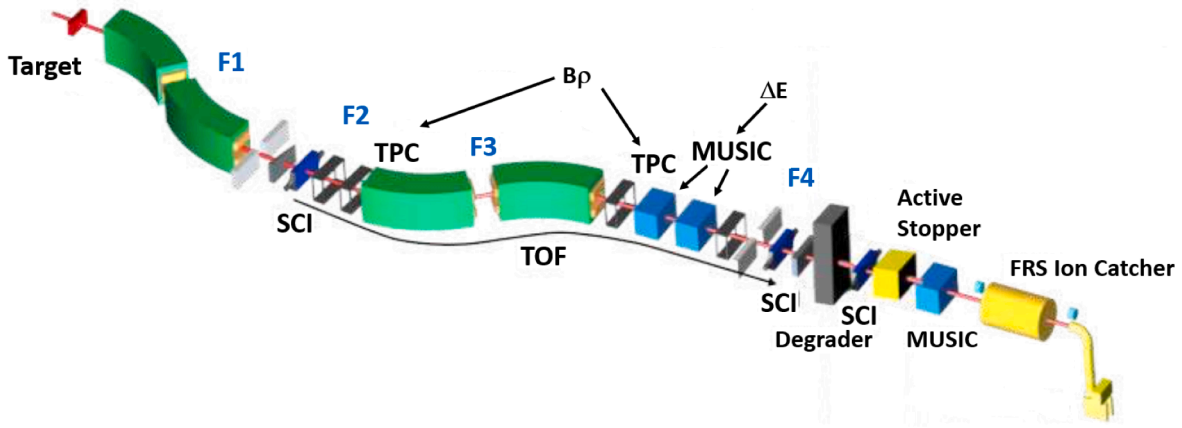

Fig. 1. Schematic view of the experimental setup of FRS from the target to the final focal plane. The F2 and F4 focal planes host the detectors used for the particle identification. The detectors at F4, downstream of the degrader, are used to monitor the implantation in either the active stopper or in the FRS Ion Catcher.

3. Data analysis

To determine the charge Q, the velocity dependence of the energy loss in the MUSIC detector gas was calibrated using the primary beam at five different energies. A linear scaling was applied to align the charge peaks. After combining all the settings, charge identification could be done, enabling an unambiguous validation using the ^{208}Pb primary beam, its charge states, and the fragment settings.

The fragments were produced using a sufficiently high primary-beam energy so that most of them were fully ionised after passing through the Nb backing of the target. However, there is a probability that the ions will capture atomic electrons when passing through matter. In addition to fully-ionised fragments throughout the entire setup (denoted 0-0, bare ion between the target and F2, and bare ion between F2 and F4), three other cases have to be taken into account, i.e., the probability of having hydrogen-like ions only in the first section of the spectrometer (denoted 1-0), only in the second section of the spectrometer (denoted 0-1), and finally the probability of ion picking up an electron inside the F4 detectors. Simulations were performed with the program GLOBAL [19] for each element studied. For ^{205}Au and ^{190}Lu one obtains 7% and 3.5% (1-0), 13% and 5.7% (0-1), and finally 16% and 6.5% probability of an electron pickup in the F4 detectors, respectively. The two-electron pick-up probability is negligible (few 0.01%) at the beam energy of the present experiment.

The charge state of the ion inside the spectrometer can be determined by measuring the horizontal (x) position of the ion at F4 with respect to the energy loss in the MUSIC. Since different charges have different trajectories in FRS they are spatially separated at F4. An example is shown in Fig. 2 (a). To identify the cases where the ion picked up an electron in MUSIC, the energy loss was measured with two MUSICs separately, with a Nb stripper foil mounted in between them to reach the charge-state equilibrium. In cases where the two charges were different, the maximum value was used to determine the Z of the ion.

A high-intensity primary beam, at the end of the calibration runs, caused damage to the F2 and F4 plastic scintillators which went unnoticed during the experiment. The standard identification procedure therefore had to be modified to account for the effect on the plastic scintillators used for time-of-flight measurements and for generating the data acquisition trigger. A detailed discussion of the applied corrections is given in Rösch-Kabadayı [20]. Fig. 2 (b) presents the A/Q spectrum for the ^{190}Lu setting before applying the corrections. The spectrum shows an offset in the A/Q determination and an unexpected curve in the charge–A/Q correlation, while the dashed line indicates the expected behaviour.

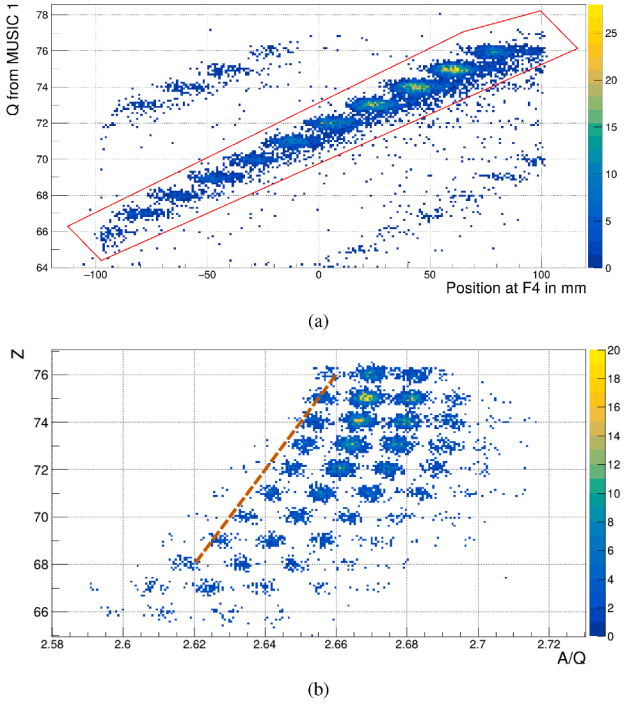

Fig. 2. (a) Q from first MUSIC plotted as function of the x position at F4. Three diagonal bands represent, from top to bottom, (1-0), (0-0) and (0-1) charge states respectively. Selection of (0-0) is shown. (b) Particle identification plot for the ^{190}Lu setting using time of flight calibration parameters. The orange line indicates the expected position of the Z-1, A-3 isotope sequence starting from ^{202}Os.

This deviation was traced back to a position-dependent timing response of the F4 scintillator, which introduces a systematic distortion in the A/Q determination. The calculated A/Q was corrected by applying two quadratic functions—one for each side of the scintillator—derived using a LISE^{++} simulation [21]. The correction functions were determined for the ^{193}W setting and subsequently applied without modification to the ^{205}Au, ^{192}Ta, and ^{190}Lu settings.

In addition to the quadratic calibration the A/Q values needed to be shifted by an ad-hoc offset. To determine this offset, applied consistently to all settings, and to properly anchor the A/Q spectra of the three settings, the following procedure was adopted. The offset was extracted by comparing the identification pattern of the ^{193}W setting with the corre-

Table 1
Number of events for twelve nuclides detected in the ^{190}Lu setting, listed for different gating combinations. The gating conditions listed are as follows: (1) Charge-state selection, correction, and calibration; (2) vertical position gates at the intermediate F2 focus to reduce pile-up; (3) time gate on the TPC delay-line signals to select realistic events; gate (4) selects events in which the horizontal position at F2 as calculated from the TPC information matches the values from the F2 scintillator. Several isotopes of Tm are displayed to illustrate how the gating condition affect counting statistic.

Condition	^{181}Tm	^{182}Tm	^{183}Tm	^{184}Tm	^{191}Lu	^{193}Hf	^{195}Ta	^{196}Ta	^{198}W	^{199}W	^{200}Re	^{201}Re
(1)	91	41	7	5	1	4	36	5	27	2	91	12
(1)+(2)	89	38	6	5	1	3	30	3	19	2	80	8
(1)+(2)+(3)	84	32	6	5	0	1	27	3	17	2	75	7
(1)+(2)+(4)	82	35	5	4	0	2	25	2	14	2	71	8
(1)+(2)+(3)+(4)	79	30	5	**4**	0	1	**23**	2	**14**	2	**68**	**7**

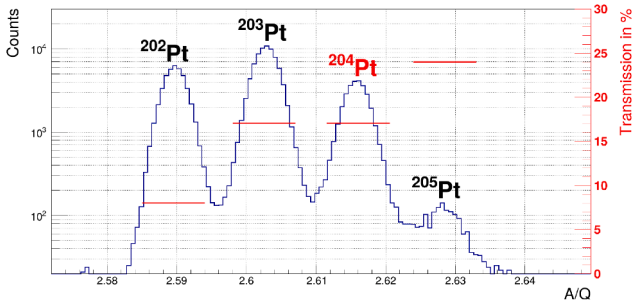

Fig. 3. A/Q values observed for the isotopes of Pt produced with the ^{193}W setting. The LISE^{++} simulation gives a transmission of 8% for ^{202}Pt, 17% for the ^{203}Pt and ^{204}Pt and 24% for the ^{205}Pt, marked in red in the plot. The sharp decrease in yield between two adjacent peaks identifies the position of the $N = 126$ line. See text for details.

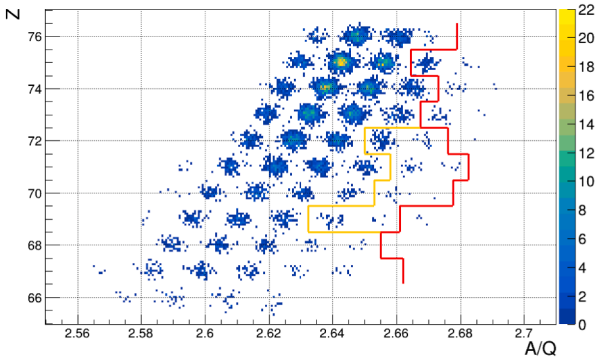

Fig. 4. The particle identification plot for the ^{190}Lu setting after the corrections on the scintillators at F2 and F4 have been applied. The red line shows the boundary of new isotopes in 2025, while the orange line indicates the discovery limits in 2020[22].

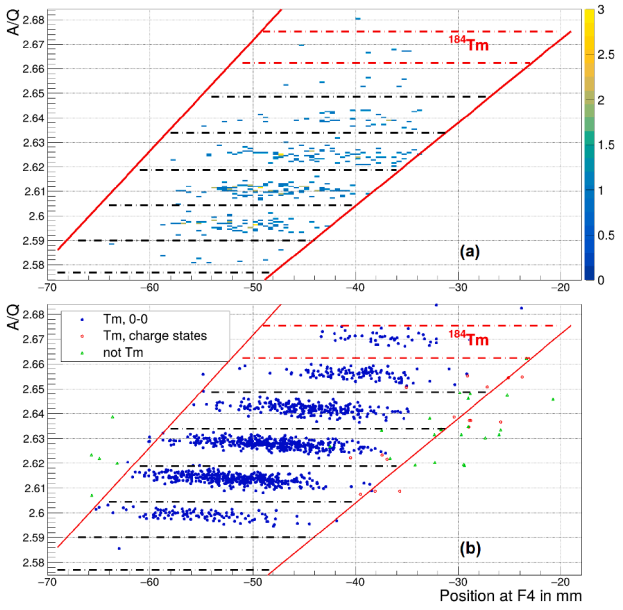

Fig. 5. (a) A/Q versus position at F4 showing the selection gates used to select and count the individual isotopes of Tm in the ^{190}Lu setting. See text for detail. (b) A simulation result using MOCADI [27] including charge states of Tm and neighboring isotopes is also shown. It includes fully ionized Tm isotopes (plain blue circles), Tm charge states (empty red circles), and other contaminants from charge states of neighboring elements (green triangles).

sponding LISE^{++} simulation results. The reference was the $N = 126$ isotonic line for Pt isotopes. In the fragmentation of ^{208}Pb, the production of nuclei beyond $N = 126$ requires hadronic processes such as Δ excitation, leading to a significantly reduced cross section. As illustrated in Fig. 3, the position of ^{204}Pt can therefore be inferred from the observed yield distribution. The same offset was then applied to the remaining settings. Independent confirmation of the mass identification was obtained using the FRS ion catcher and its mass-tagging capability [23,24]. Fig. 4 shows the identification plot (Z vs. A/Q) for the ^{190}Lu setting after integrating those corrections.

4. Results and discussion

Fig. 5 (a) shows the gates in A/Q vs. position at F4 that were used to select and count the individual Tm isotopes. The spectrum is displayed after applying the charge-state selection and the Z selection as well as the gates listed in Table 1. Similar plots are present in Rösch-Kabadayı [20] for Ta, W, and Re. The continuous red line limits the position acceptance of the isotope based on the LISE^{++} simulation, the dotted-dashed lines show the isotope selections (red for the reported isotopes). As illustrated in Fig. 5 (a), the distribution of the observed events is located inside of the phase space of the focal plane for given isotopes. Fig. 5 (b) shows a simulation with higher statistics of contaminants illustrating that other species would not fit in the same positions. In Table 1, the numbers of events consistent with nine isotopes that were not discovered when the data was collected using different gating conditions are listed together with three isotopes of Tm to illustrate the effect of the gating conditions. Selection conditions (2) and (3) help reduce pile-up events, usually used in high intensity conditions. Condition (4) is a stringent consistency check between projected position measured in the TPC and that obtained using a narrow gate on the time difference of the photomultiplier of the F2 plastic.The A/Q, position at F4, and Z remain within the same narrow range when the different selection criteria are applied.

In the literature, the detection of three events is considered sufficient to mark the unambiguous observation of an isotope [25,26]. Us-

ing this criterion, we identify five isotopes that have been recently published [12]. In the cases of ^{191}Lu, ^{195}Hf, ^{196}Ta and ^{199}W some events are observed, but their number is insufficient for discovery, in particular when taking stricter selection gates into account. The determination of production cross sections from the present data requires a better understanding of the behaviour and efficiency of the plastic scintillator at the F4 focal plane. Measured counts exhibit a position-dependent attenuation relative to LISE^{++} simulations. The shape of this position dependent efficiency is consistent, within statistical error, between the ^{193}W and the ^{190}Lu settings. Therefore, a more detailed analysis is currently underway and will be presented in a forthcoming publication.

5. Summary and conclusions

The ^{184}Tm, ^{195}Ta, ^{198}W, ^{200}Re, and ^{201}Re isotopes were produced in the fragmentation of a 1.05 GeV/nucleon ^{208}Pb beam in an experiment at the GSI fragment separator FRS. These observations are in line with the most recent extension of the nuclear chart and highlight the capabilities of the FRS and in-flight fragmentation at relativistic energies in accessing this region. The isotope ^{201}Re is a particularly significant discovery as it lies directly on the $N = 126$ line, marking a critical point towards the *r*-process path and providing valuable input for nuclear structure and astrophysical models. Those five isotopes were reported in the 2025 dissertation by Heidi Rösch-Kabadayi [20] and this manuscript summarizes this finding. They are also contained in the set of newly identified nuclides in the recently published work by Fukuda et al. [12]. The experiment therefore demonstrates that the FRS is competitive with modern facilities making the impending arrival of the new separator Super-FRS [28] at FAIR with beam intensities increasing up to a factor 100 an exciting prospect.

Declaration of competing interest

The authors declare that they have no known competing financial interests or personal relationships that could have appeared to influence the work reported in this paper.

Acknowledgements

The results presented here are based on the experiment S468, which was performed at the FRS at the GSI Helmholtzzentrum für Schwerionenforschung, Darmstadt (Germany) in the context of FAIR Phase-0. This work was supported by the German Federal Ministry of Research, Technology and Space (BMFTR) under contract nos. 05P19RGFN1, 05P19RDFN1, 05P21RDFN1, and 05P24RG1, by HGS-HIRe and by the strategic Helmholtz partnership agreements between GSI and Justus-Liebig-Universität Gießen as well as GSI and TU Darmstadt. TKN and SP acknowledge support from Grant PID2023-147569NB-C21, funded by MICIU/AEI/10.13039/501100011033, Spain, and ERDF, UE and the GSI-IN2P3-DRF agreement under number 22-88. AMB, CEJ, ZP and PHR acknowledge support from the UK Science and Technology Facilities Council grant nos. ST/L005743/1, ST/P003982/1, ST/P005314/1 and ST/V001108/1. SASA acknowledges support from the German Research Foundation (DFG) under Contract No. AY 155/2-1. AK acknowledges funding from the European Union's Horizon 2020 research and innovation programme under Grant Agreement No. 771036 (ERC CoG MAIDEN) and from the Research Council of Finland under the project No. 354968. PHR acknowledges support from the National Measurements System programmes unit of the UK department for Science, Innovation and Technology. JLRS. acknowledges support from Xunta de Galicia under the program of postdoctoral fellowships ED481B-2017-002 and ED481D-2021-018. This work was supported by the Slovenian Research and Innovation Agency through grant Nos. I0-E005 and P1-0102. NK acknowledges the support of ExtreMe Matter Institute EMMI at the GSI Helmholtzzentrum für Schwerionenforschung, Germany.

Data availability

Data will be made available on request.

References

[1] M. Arnould, S. Goriely, K. Takahashi, The r-process of stellar nucleosynthesis: astrophysics and nuclear physics achievements and mysteries, Phys. Rep. 4 (2007) 97–213. https://doi.org/10.1016/j.physrep.2007.06.002

[2] J.J. Cowan, C. Sneden, J.E. Lawler, A. Aprahamian, M. Wiescher, K. Langanke, G. Martínez-Pinedo, F.-K. Thielemann, Origin of the heaviest elements: the rapid neutron-capture process, Rev. Mod. Phys. 93 (2021) 015002. https://doi.org/10.1103/RevModPhys.93.015002

[3] B.P. Abbot, et al., Multi-messenger observations of a binary neutron star merger, Astrophys. J. Lett. 848 (2017) L12. https://doi.org/10.3847/2041-8213/aa91c9

[4] Y.W. Hao, Y.F. Niu, Z.M. Niu, Sensitivity of the r-process rare-earth peak abundances to nuclear masses, Phys. Lett. B 844 (2023) 138092. https://doi.org/10.1016/j.physletb.2023.138092

[5] I.V. Panov, Y.S. Lutostansky, F.-K. Thielemann, Beta-decay half-lives for the r-process nuclei, Nucl. Phys. A 947 (2016) 1–11. https://doi.org/10.1016/j.nuclphysa.2015.12.001

[6] T. Otsuka, A. Gade, O. Sorlin, T. Suzuki, Y. Utsuno, Evolution of shell structure in exotic nuclei, Rev. Mod. Phys. 92 (2020) 015002. https://doi.org/10.1103/RevModPhys.92.015002

[7] J. Kurcewicz, F. Farinon, H. Geissel, S. Pietri, C. Nociforo, A. Prochazka, H. Weick, J.S. Winfield, A. Estradé, P.R.P. Allegro, A. Bail, G. Bélier, J. Benlliure, G. Benzoni, M. Bunce, M. Bowry, R. Caballero-Folch, I. Dillmann, A. Evdokimov, J. Gerl, A. Gottado, E. Gregor, R. Janik, A. Kelić-Heil, R. Knöbel, T. Kubo, Y.A. Litvinov, E. Merchan, I. Mukha, F. Naqvi, M. Pfützner, M. Pomorski, Z. Podolyák, P.H. Regan, B. Riese, M.V. Ricciardi, C. Scheidenberger, B. Sitar, P. Spiller, J. Stadlmann, P. Strmen, B. Sun, I. Szarka, J. Taïeb, S. Terashima, J.J. Valiente-Dobón, M. Winkler, P. Woods, Discovery and cross-sectiom measurment of neutron-rich isotopes in the element range from neodynium to platinum with the FRS, Phys. Lett. B 717 (2012) 371–375. https://doi.org/10.1016/j.physletb.2012.09.021

[8] K.-H. Schmidt, K. Sümmerer, H. Geissel, G. Münzenberg, F. Nickel, M. Pfützner, M. Weber, B. Voss, T. Brohm, H.-G. Clerc, M. Fauerbach, J.-J. Gaimard, A. Grewe, E. Hanelt, M. Steiner, J. Weckenmann, C. Ziegler, A. Magel, Proton removal in peripheral nuclear collisions at relativistic energies, Nucl. Phys. A 542 (4) (1992) 699–714. https://doi.org/10.1016/0375-9474(92)90264-K

[9] J. Benlliure, K.-H. Schmidt, D. Cortina-Gil, T. Enqvist, F. Farget, A. Heinz, A.R. Junghans, J. Pereira, J. Taieb, Production of neutron-rich isotopes by cold fragmentation in the reaction 197Au + Be at 950 A MeV, Nucl. Phys. A 660 (1) (1999) 87–100. https://doi.org/10.1016/S0375-9474(99)00386-3

[10] C. Gaarde, Isobar excitations in nuclei, Annu. Rev. Nucl. Part. Sci. 41 (1991) 187–218. https://doi.org/10.1146/annurev.ns.41.120191.001155

[11] T. Niwase, Y.X. Watanabe, Y. Hirayama, M. Mukai, P. Schury, A.N. Andreyev, T. Hashimoto, S. Iiruma, H. Ishiyama, Y. Ito, S.C. Jeong, D. Kaji, S. Kimura, H. Miyatake, K. Morimoto, J.-Y. Moon, M. Oyaizu, M. Rosenbusche, A. Taniguchi, M. Wada, Discovery of new isotope 241U and systematic high-precision atomic mass measurements of neutron-rich Pa-Pu nuclei produced via multinucleon transfer reactions, Phys. Rev. Lett. 130 (2023) 132502. https://doi.org/10.1103/PhysRevLett.130.132502

[12] N. Fukuda, S. Michimasa, H. Suzuki, Y. Shimizu, H. Takeda, Y. Togano, M. Yoshimoto, Y. Yanagisawa, K. Kusaka, M. Ohtake, H. Sato, T. Sumikama, K. Yoshida, S. Motomura, H. Baba, Y. Ichonohe, N. Kitamura, K.G. Tanaka, K. Kasai, D. Suzuki, N. Imai, R. Yokoyama, Y. Yamamoto, S. Hanai, Y. Funasaka, R. Tsuchiya, N. Matsuoka, N. Fukunishi, H. Sakurai, First observation of twenty-two exotic isotopes using a ^{208}Pb primary beam at RIBF, Prog. Theor. Exp. Phys. (2026) 061D01. https://doi.org/10.1093/ptep/ptag082

[13] H. Geissel, P. Armbruster, K.H. Behr, A. Brünle, K. Burkard, M. Chen, H. Folger, B. Franczak, H. Keller, O. Klepper, B. Langenbeck, F. Nickel, E. Pfeng, M. Pfützner, E. Roeckl, K. Rykaczewski, I. Schall, D. Schardt, C. Scheidenberger, K.-H. Schmidt, A. Schröter, T. Schwab, K. Sümmerer, M. Weber, G. Münzenberg, T. Brohm, H.-G. Clerc, M. Fauerbach, J.-J. Gaimard, A. Grewe, E. Hanelt, B. Knödler, M. Steiner, B. Voss, J. Weckenmann, C. Ziegler, A. Magel, H. Wollnik, J.P. Dufour, Y. Fujita, D.J. Vieira, B. Sherrill, The GSI projectile fragment separator (FRS): a versatile magnetic system for relativistic heavy ions, Nucl. Instrum. Methods Phys. Res. B: Beam Interact. Mater. At. 70 (1-4) (1992) 286–297. https://doi.org/10.1016/0168-583X(92)95944-M

[14] M. Pfützner, H. Geissel, G. Münzenberg, F. Nickel, C. Scheidenberger, K.-H. Schmidt, K. Sümmerer, T. Brohm, B. Voss, H. Bichsel, Energy deposition by relativistic heavy ions in thin argon absorbers, Nucl. Instrum. Methods Phys. Res. B:Beam Interact. Mater. At. 86 (1994) 213–218. https://doi.org/10.1016/0168-583X(94)95280-9

[15] R. Janik, A. Prochazka, B. Sitar, P. Strmen, I. Szarka, H. Geissel, K.-H. Behr, C. Karagiannis, C. Nociforo, H. Weick, M. Winkler, Time projection chambers with C-pads for heavy ion tracking, Nucl. Instrum. Methods Phys. Res. A: Accel. Spectrom. Detect. Assoc. Equip. 640 (2011) 54–57. https://doi.org/10.1016/j.nima.2011.02.052

[16] W.R. Plaß, T. Dickel, S. Purushothaman, P. Dendooven, H. Geissel, J. Ebert, E. Haettner, C. Jesch, M. Ranjan, M.P. Reiter, H. Weick, F. Amjad, S. Ayet, M. Diwisch, A. Estrade, F. Farinon, F. Greiner, N. Kalantar-Nayestanaki, R. Knöbel, J. Kurcewicz, J. Lang, I. Moore, I. Mukha, C. Nociforo, M. Petrick, M. Pfützner, S. Pietri, A. Prochazka, A.-K. Rink, S. Rinta-Antila, D. Schäfer, C. Scheidenberger, M. Takechi, Y.K. Tanaka, J.S. Winfield, M.I. Yavor, The FRS ion catcher – a facility for high-precision experiments with stopped projectile and fission fragments, Nucl.

Instrum. Methods Phys. Res. B: Beam Interact. Mater. At. 317 (2013) 457–462. https://doi.org/10.1016/j.nimb.2013.07.063

[17] R. Kumar, F.G. Molina, S. Pietri, E. Casarejos, A. Algora, J. Benlliure, P. Doornenbal, J. Gerl, M. Gorska, I. Kojouharov, Z. Podolyák, W. Prokopowicz, P.H. Regan, B. Rubio, H. Schaffner, S. Tashenov, H.-J. Wollersheim, Testing of a DSSSD detector for the stopped RISING project, Nucl. Instrum. Methods Phys. Res. A: Accel. Spectrom. Detect. Assoc. Equip. 598 (3) (2009) 754–758. https://doi.org/10.1016/j.nima.2008.08.155

[18] T. Dickel, C. Hornung, D. Amanbayev, S. Ayet San Andrés, S. Beck, J. Bergmann, H. Geissel, J. Gerl, M. Górska, L. Gröf, E. Haettner, J.-P. Hucka, D.A. Kostyleva, G. Kripko-Koncz, A. Mollaebrahimi, I. Mukha, S. Pietri, W.R. Plass, Z. Podolyák, S. Purushothaman, M.P. Reiter, H. Roesch, C. Scheidenberger, Y.T. Tanaka, H. Weick, J. Zhao, Super-FRS-Experiment-Collaboration, Mean range bunching of exotic nuclei produced by in-flight fragmentation and fission - stopped-beam experiments with increased efficiency, Nucl. Instrum. Methods Phys. Res. B: Beam Interact. Mater. At. 541 (1) (2023) 275–278. https://doi.org/10.1016/j.nimb.2023.05.018

[19] C. Scheidenberger, T. Stoehlker, W. Meyerhof, H. Geissel, P.H. Mokler, B. Blank, Charge states of relativistic heavy ions in matter, Nucl. Instrum. Methods Phys. Res. B: Beam Interact. Mater. At. 142 (1998) 441. https://doi.org/10.1016/S0168-583X(98)00244-4

[20] H.A. Rösch-Kabadayı, Production and Identification of New Neutron-Rich Isotopes Close to the N = 126 Line at the Fragment Separator of GSI, Ph.D. thesis, Technische Universität Darmstadt, 2025. https://doi.org/10.26083/tuprints-00031406

[21] O.B. Tarasov, D. Bazin, LISE++: exotic beam production with fragment separators and their design, Nucl. Instrum. Methods Phys. Res. B: Beam Interact. Mater. At. 376 (2016) 185–187. https://doi.org/10.1016/j.nimb.2016.03.021

[22] M. Thoennessen, Discovery of Nuclides Project, 2026, Accessed: 2026-12-01, https://people.frib.msu.edu/thoennes/isotopes/.

[23] C. Hornung, T. Dickel, D. Amanbayev, S. Ayet San Andrés, D.L. Balabanski, S. Beck, J. Bergman, P. Constantin, J. Erbert, H. Geissel, F. Greiner, L. Gröf, E. Haettner, M.N. Harakeh, J.-P. Hucka, N. Kalantar-Nayestanaki, D.A. Kostyleva, G. Kripko-Koncz, I. Miskun, A. Mollaebrahimi, I. Mukha, G. Münzenberg, S. Pietri, W.R. Plaß, S. Purushotaman, M.P. Reiter, A.-K. Rink, H. Roesch, C. Scheidenberger, A. Spataru, Y.K. Tanaka, H. Weick, J. Zhao, Mass tagging: verification and calibration of particle identification by high-resolution mass measurments, Nucl. Instrum. Methods Phys. Res. B 541 (2023) 257. https://doi.org/10.1016/j.nimb.2023.04.045

[24] D. Amanbayev, Mass Measurments at the N = Z and N = 126 Limits at the FRS Ion Catcher and Development of the Cryogenic Stopping Cell for the Super-FRS, Ph.D. thesis, Justus-Liebig-Universität Gießen, 2023. https://doi.org/10.22029/jlupub-18567

[25] K. Haak, O.B. Tarasov, P. Chowdhury, A.M. Roggers, K. Sharma, T. Baumann, D. Bazin, P.C. Bender, J. Chen, A. Estrade, M.A. Famiano, D.C. Foulds-Holt, N. Fukuda, A. Gade, T.N. Ginter, R.W. Gohier, M. Hausmann, A.M. Hill, D.E.M. Hoff, L. Klankowski, E. Kwan, J. Li, S.N. Liddick, B. Longfellow, S. Lyons, C. Morse, M. Portillo, D. Rhodes, A.L. Richard, S. Samaranayake, B.M. Sherill, M.K. Smith, M. Spieker, C.S. Sumithrarachchci, H. Suzuki, K. Wang, S. Waniganeththi, D. Weisshaar, S. Zhu, Production and discovery of neutron-rich isotopes by fragmentation of ^{198}Pt, Phys. Rev. C 108 (2023) 034608. https://doi.org/10.1103/physrevc.108.034608

[26] O.B. Tarasov, A. Gade, K. Fukushima, M. Haussmann, E. Kwan, M. Portillo, M. Smith, D.S. Ahn, D. Bazin, R. Chyzh, S. Giraud, K. Haak, T. Kubo, D.J. Morrisey, P.N. Ostroumov, I. Richardson, B.M. Sherrill, A. Stoltz, S. Watters, D. Weisshaar, T. Zhang, Observation of new isotopes in fragmentation of ^{198}Pt at FRIB, Phys. Rev. Lett. 132 (2024) 072501. https://doi.org/10.1103/physrevlett.132.072501

[27] N. Iwasa, H. Weick, H. Geissel, New features of the Monte Carlo code MOCADI, Nucl. Instrum. Methods Phys. Res. B 269 (2011) 752. https://doi.org/10.1016/j.nimb.2011.02.007

[28] H. Geissel, M. Weick, M. Winkler, et al., The super-FRS project at GSI, Nucl. Instrum. Methods Phys. Res. B: Beam Interact. Mater. At. 204 (2003) 71–85. https://doi.org/10.1016/S0168-583X(02)01893-1